EGG-M-23982

Conf-830301--15

THERMAL PERFORMANCE OF A GEOFLUID DIRECT-CONTACT HEAT EXCHANGER

EGG-M--23982

DE82 013233

to be presented at the session
on Two-Phase Flow and Boiling Heat Transfer
ASME-JSME Thermal Engineering Joint Conference

By D. J. Wiggins, G. L. Mines, E. Wahl

Abstract

A sieve-tray direct-contact heat exchanger was used to transfer heat from a 280°F geothermal fluid to the working fluid, isobutane, in the Raft River 60kW prototype plant. A series of experiments were run at different working fluid-to-geofluid flow ratios which produced different boiling conditions. In this paper, the results of these experiments are analyzed on the basis of thermal performance. The flow ratio, the geofluid outlet temperature, the working fluid inlet temperature, the amount of working fluid dissolved or entrained in geofluid, and tray efficiency are varied and preheating temperature profiles are calculated. These are compared with the experimentally obtained temperature profiles and the relative effects of the variables are evaluated. From this, it was determined that the approach temperature difference was on the order of .1° after 17 preheating trays, and the tray efficiencies, which appear to be about the same for all trays, reached approximately 70 percent. It was also determined that entrainment has a negligible effect on column thermal performance. The thermal performance of this column compares favorably with a spray-tower direct-contact heat exchanger and a shell-and-tube heat exchanger in terms of overall heat-transfer coefficient. Distributor tray and boiling tray behavior are discussed. There is some discussion of operations and thermal hydraulics as well.

DISCLAIMER

Introduction

As part of the Department of Energy's Geothermal Conversion Technology effort, a specially designed sieve plate direct contact heat exchanger (DCHX) was tested in the 60 kW prototype test plant which is located in the Raft River Valley (RR) of Southern Idaho. The prototype plant is used to test components and/or different systems or cycles to produce electrical power from the low-temperature geothermal fluid (280°F) available at the site. Isobutane was used as the working fluid.

A flow schematic of the plant showing the components which are necessary for direct contact operation in a binary cycle is depicted in Figure 1. Since the geofluid and working fluid are in physical contact with one another, it is necessary to boost the pressure of both fluids to the direct contact column operating pressure using the geofluid boost pump and working fluid boost and feed pumps. The geofluid enters the column at the top and flows out the bottom, preheating and vaporizing the working fluid which flows in the bottom as a liquid and out the top as a vapor. The working fluid may also be withdrawn before it begins to boil in order to simulate a separate preheater unit in a multiple heater cycle. The effluent geofluid is then discharged to a holding pond prior to reinjection. The working fluid vapor can be expanded either through the turbine which drives a generator to produce electrical power or through the turbine by-pass valve which drops the vapor pressure prior to its entering the condenser. In the condenser, the vapor is desuperheated and condensed, and the condensate is pumped back into the direct contact for another heat exchange cycle. The turbine was part of prior tests with the plant and could not be used for the direct contact testing without modifications to reduce flow area. A different working fluid could have been used but would have resulted in poor performance for this resource temperature. The vent condenser and preflasher unit are used to decrease the effect of noncondensibles in the geofluid. The noncondensibles increase the pressure in the condenser and decrease the rate of condensation. The vent condenser minimizes working fluid losses by recovering most of the isobutane when the noncondensibles are vented to the atmosphere. The preflasher unit removes noncondensibles from the geofluid before it enters the system by flashing the geofluid at a lower pressure.

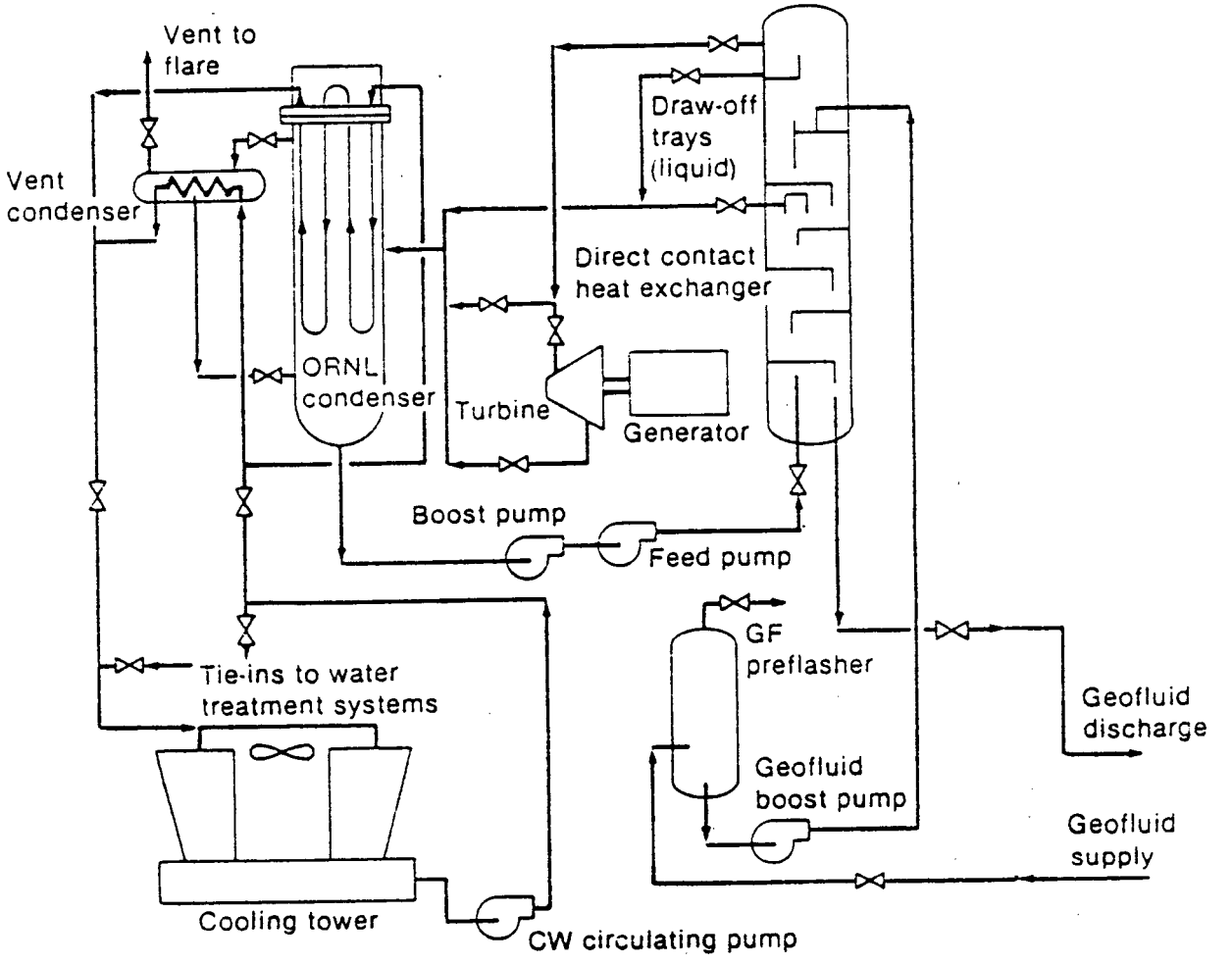

FIGURE 1. Prototype Flow Schematic

The purpose of testing this system is to evaluate the use of a sieve plate direct contact heat exchanger in a geothermal binary cycle. The direct contact heat exchanger does not have problems with fouling on heat transfer surfaces and can handle corrosive geofluid without the expense of the special materials which would be needed in an ordinary shell and tube heat exchanger. The sieve plate type of direct contact heat exchanger was chosen because the mass and heat transfer can be better controlled than in a spray type.

Column Thermal Hydraulics

The sieve plate direct contact heat exchanger is approximately 19½ feet tall with a 1-foot diameter. The internals of the column are depicted in Figure 2. The working fluid enters the bottom of the column and flows up through the holes in the 19 plates and leaves the top of the column as a saturated or slightly superheated vapor. The 1/8-inch sized holes in the plates cause the working fluid to disperse as evenly sized droplets into the continuous geofluid phase and then to coalesce into layers of varying thickness of working fluid under each plate. By repeatedly reforming the drops, a higher temperature difference between the geofluid and drop surface is maintained, and the average temperature of the dispersed working fluid more quickly approaches the temperature of the continuous geofluid. Although the two fluids are fairly insoluble and the rate of heat transfer is faster than the rate of mass transfer, some working fluid is entrained/dissolved and lost. It is desirable to minimize this loss by minimizing the contact time of the two fluids, since the loss penalizes the economics. Only this type of unflooded flow pattern will be addressed here.

In this application, a tray is defined as the region between two plates in the column into which geofluid containing entrained working fluid flows from above and working fluid flows in the form of droplets up through the holes in the plate below. There are 17 preheating trays and two boiling trays in this column. Thermocouples and RTD's are placed at appropriate locations in these trays. The working fluid enters the column through a pipe which travels through the distributor tray area (tray 0, Figure 2) and discharges under the first plate. The geofluid flows around this pipe in the tray 0 region and exits the bottom of the column. The geofluid enters near the top of the column where it discharges onto plate 19. The working fluid vapor passes through this liquid layer and exits near the top of the column.

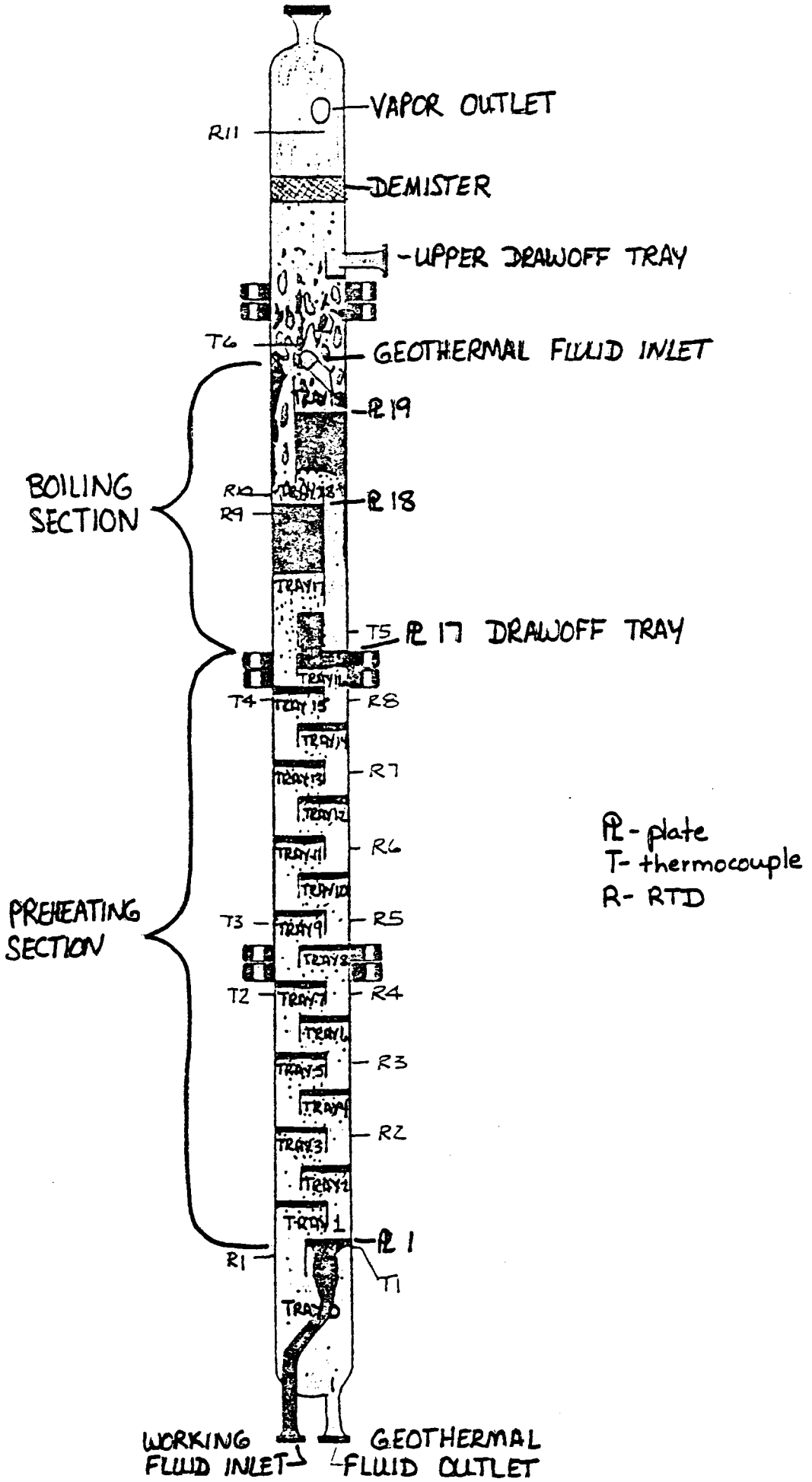

FIGURE 2. Schematic of the Internals of the Sieve Plate Direct Contact Heat Exchanger

Thermal Model

A model of the column's thermal behavior was constructed based on some knowledge of the thermal hydraulics. This was done in order to: 1) smooth the data, 2) calculate the tray efficiency, 3) better understand the thermal behavior, and 4) serve as a performance prediction tool.

In constructing this model, the fluid contact zone was visualized as is depicted in Figure 3. The average outlet working fluid to outlet geofluid flow ratio as calculated by a boiler energy balance, an overall energy balance, inlet flow rate data, and outlet flow rate data is used. Entrainments for each tray are interpolated from the entrainment at the bottom of the column (generally based on measurement) which is a user input variable.

The following assumptions were made:

1. Although contacting is crossflow so that it behaves between countercurrent and parallel, and the outflowing streams may not be thermally homogeneous, it is assumed that all outflowing streams are thermally homogeneous.

2. Working fluid is entrained in outflowing streams of geofluid and is assumed to have an enthalpy of the working fluid at the outflowing geofluid temperature.

3. The amount of working fluid which is dissolved in the outflowing geofluid is negligible.

4. Liquid geothermal fluid entrained in liquid working fluid in the column body is considered to be negligible because the geothermal is in the continuous phase in the lower portion of the column, and above the interface, the density difference is substantial with a large cross-sectional area for flow of the working fluid and low flow velocities.

5. Some water vapor is mixed with the outflowing working fluid vapor.

6. The theoretically obtainable outlet temperature for a 100% efficient tray is equal for both streams.

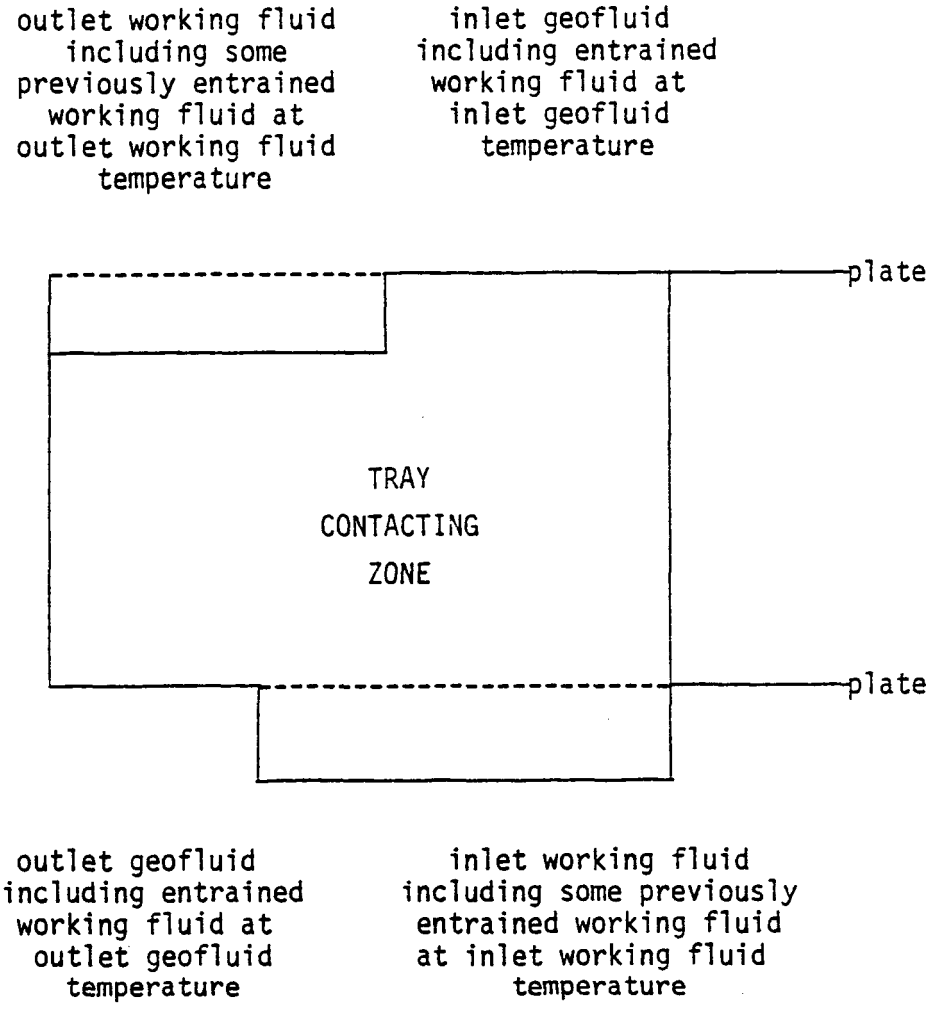

FIGURE 3. Contact Zone for Any Given Tray

The calculations in the model start at the bottom of the column at the distributor tray (tray 0) and progress through the preheater section and the boiler section using enthalpy balances and tray efficiency definition. Efficiency using either geofluid or working fluid temperature is defined as the ratio of the actual temperature difference (inlet to outlet) to the theoretical temperature difference, where the theoretical temperature difference is for a 100% efficient tray when both the working fluid and geofluid leave the tray at the same temperature. Since direct contact flow does not occur throughout the distributor tray region, the distributor tray is handled separately using three of the tray's experimentally obtained temperatures to calculate the fourth temperature and the tray efficiency. Two of these distributor tray temperatures (the geofluid inlet and the working fluid outlet temperatures), the working fluid-to-geofluid flow ratio, and the user inputted tray efficiency are then used to start the calculations for the preheater trays. Experimentally obtained temperatures are not used in the preheater section. Temperatures are generated on a tray-by-tray basis through this section using the two known temperatures from the previous tray to calculate the two unknown temperatures for the current tray. An iterative loop of enthalpy balance calculations and efficiency calculations is used to do this. The enthalpy balance includes the movement of any entrained working fluid. Two efficiency equations are used; one based on geofluid temperatures and the other based on working fluid temperatures. In order for these two efficiencies to be equal, it is assumed that the average heat capacity of the working fluid traversing the actual temperature range in a tray is equivalent to the average heat capacity of the working fluid traversing the theoretical temperature range. This is not a bad assumption given the small temperature differences which are observed in each tray. The boiling section was then treated separately using the experimental temperatures (enthalpies in this case) to calculate the efficiency of the two boiling trays.

Results

The previously described model was used to evaluate the experimentally obtained data. Seven experiments were run, six of which were evaluated. These experiments are listed in Table 1. The working fluid-to-geofluid flow ratio, and one preheater tray efficiency (used for all preheater trays) was determined

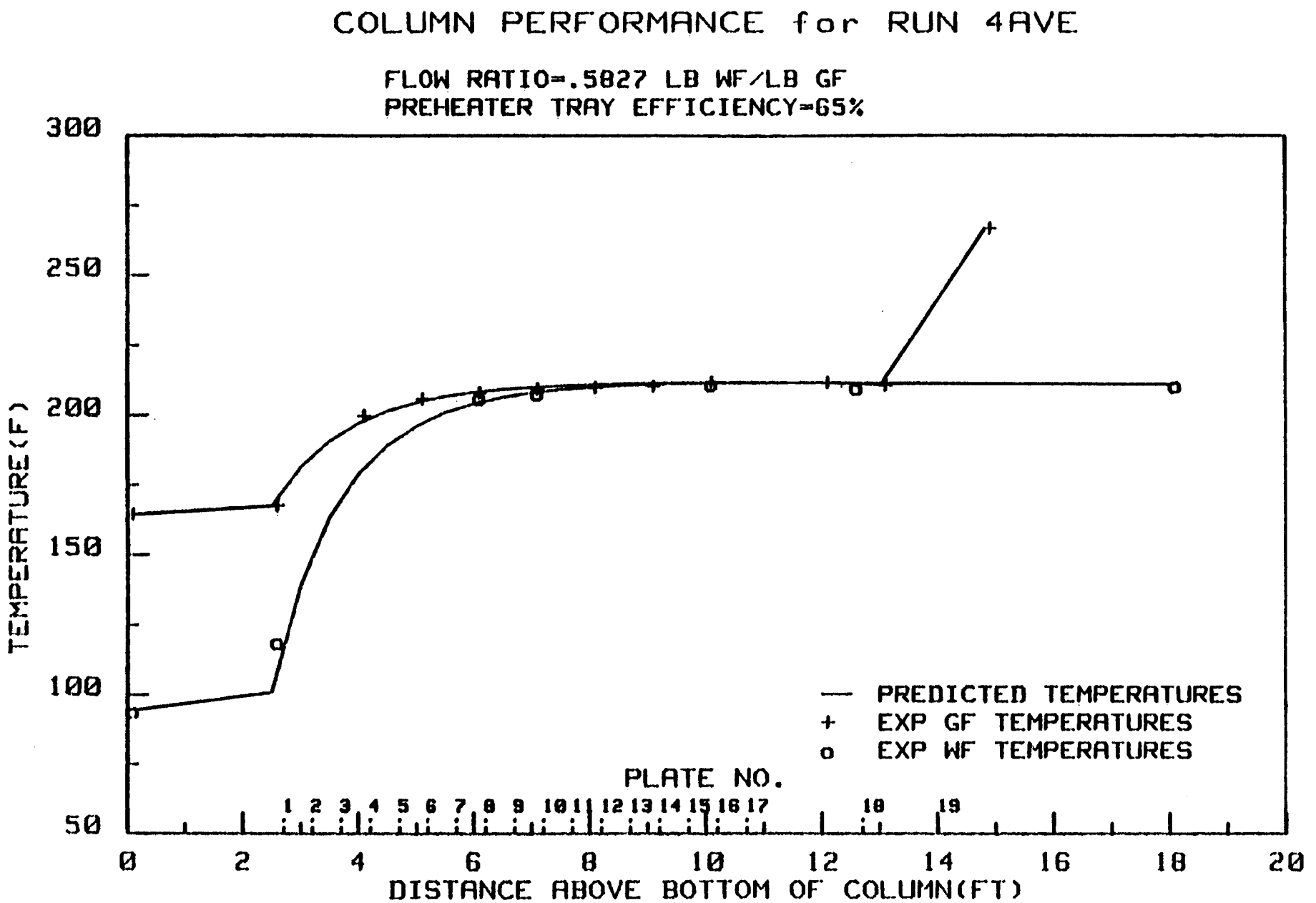

FIGURE 4. Best Curvefit of Experimental Temperatures to Predicted Values for Run 4

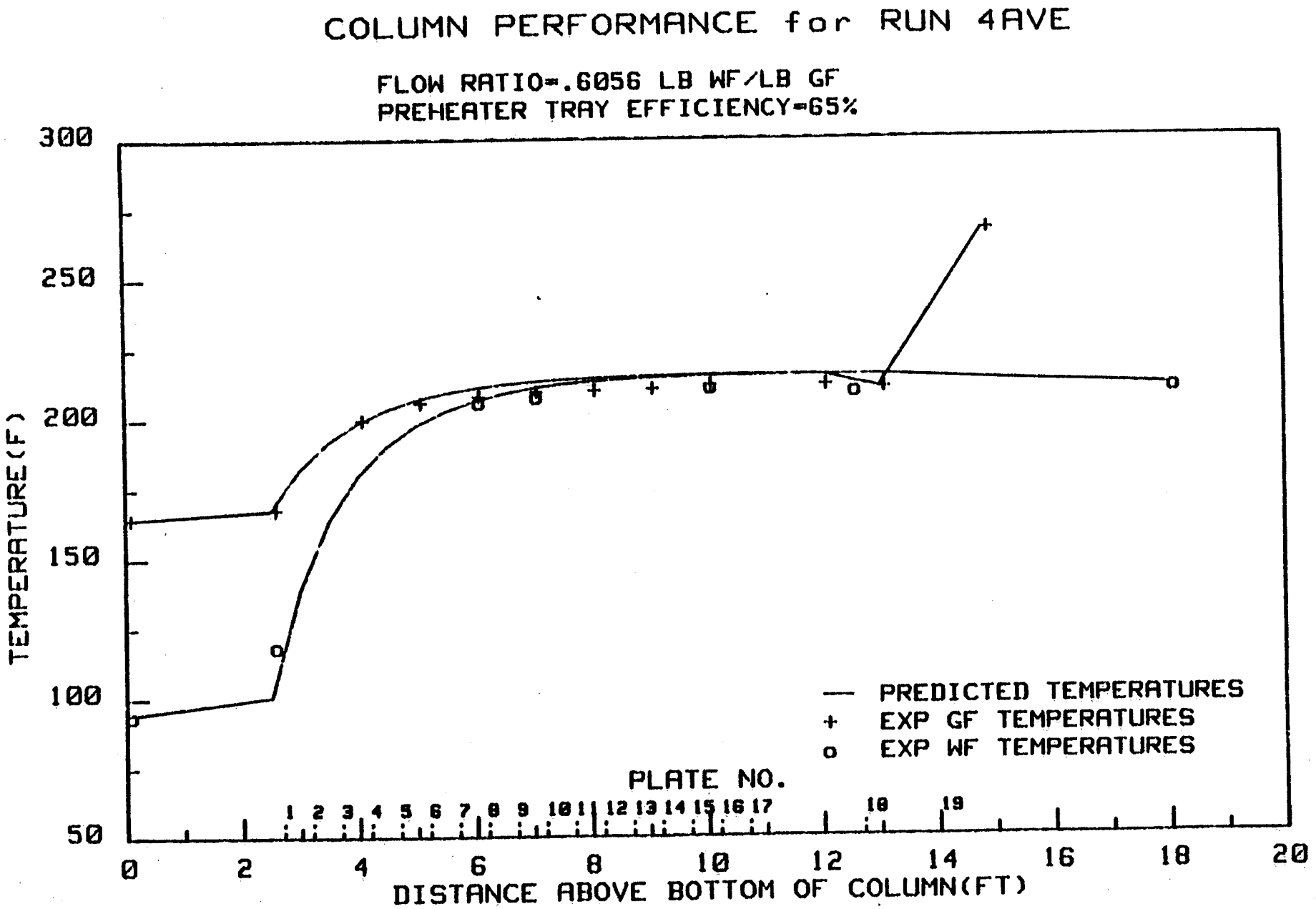

FIGURE 5. Effect of High Flow Ratio on Predicted Curve for Run 4

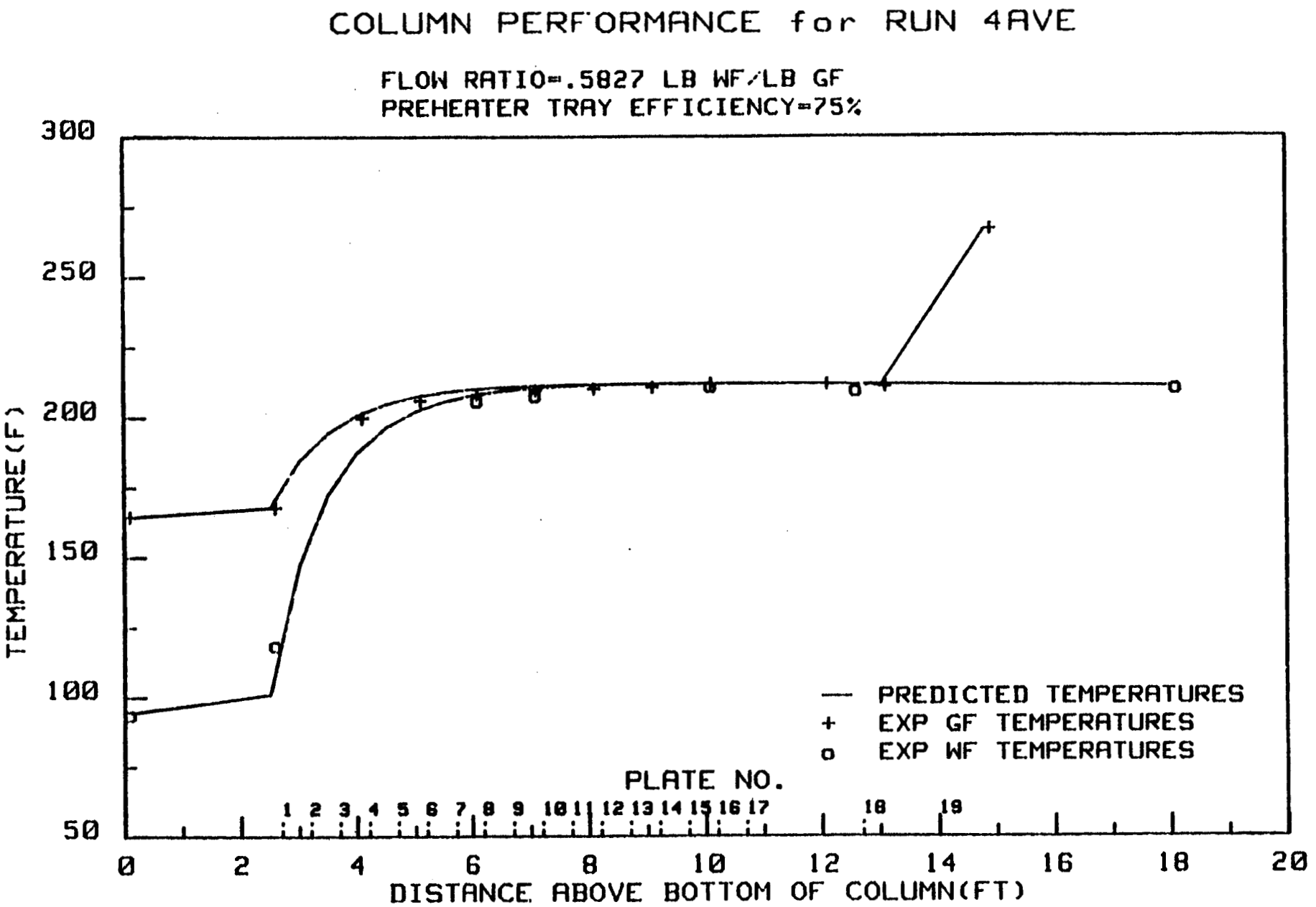

FIGURE 6. Effect of Higher Efficiency (75%) on Predicted Curve for Run 4

for each experiment by trial and error using input of working fluid-to-geofluid inlet flow ratio, and tray efficiency. The working fluid flow was varied in order to obtain the desired working fluid-to-geofluid flow ratio. This was done until the predicted temperature profile matched the experimentally obtained temperature profile within ± .1°F of the average of trays 18 and 19 outlet geofluid temperature, and the closest value to tray 8 outlet geofluid temperature. An example of the graphical output is depicted in Figure 4.

The flow ratios which best fit the experimentally obtained temperature profiles are listed in Table 2. The working fluid-to-geofluid outlet flow ratio has the largest effect on the temperatures in trays 17 and 18 (see Figure 5), whereas the preheater tray efficiency has the largest effect on trays 1-16 (see Figure 6). The working fluid entrainment in geofluid does not have a significant effect, so an experimentally obtained value of .001 $\frac{\text{lbWF}}{\text{lbGF}}$ was used. In all cases, the predicted working fluid-to-geofluid flow ratio matched the experimental flow ratio within a 10% error (see Table 2). Run 4 has the least error (.2%). This may be attributable to the highly corroded geofluid flow meters, to the oscillatory nature of the column, or to the limited accuracy of the temperature instrumentation combined with the flow instrumentation. We tried to correct for these effects by averaging several data sets. The temperature readings were specifically corrected by adjusting their values based on an isothermal temperature profile by applying individual temperature corrections determined from a calibration run in which the working fluid flow was zero and the column was isothermal.

The tray efficiencies which best fit the experimentally obtained temperature profiles are listed in Table 3. The predicted distributor tray efficiency decreases with increasing working fluid-to-geofluid flow ratio. At the lower working fluid-to-geofluid flow ratios, the layer of working fluid under plate 1 decreases so that the working fluid is forced from the tube through a thicker layer of geofluid from which more heat is transferred. Note that the working fluid temperature underneath plate 1 is always higher than expected for the working fluid. This is because of the positioning of the thermocouple so that depending on the thickness of the working fluid layer under this plate, the geofluid temperature is recorded rather than the working fluid temperature. This phenomenon is reflected in the amount of heat transfer and the overall heat transfer coefficients which are listed for the distributor region in Table 3.

The predicted preheater tray efficiency increases with increasing flow ratio (Table 3) but never exceeds the design tray efficiency of 70%. The preheater tray efficiency would increase even more rapidly with an increase in flow ratio if only the effective geofluid volume were considered (heat transfer only occurs when the working fluid bubbles through a portion of the continuous geofluid phase and this volume decreases with an increase in flow ratio). The increase in preheater efficiency is probably related to an increase in heat transfer surface area per unit mass of working fluid at high flow ratios. At high flow ratios, jetting of the working fluid through the holes in the plate occurs, causing the droplet size to decrease and the amount of heat transfer to increase. This increase in tray efficiency does not show in the overall heat transferred or in the heat transfer coefficient shown in Table 3; it is masked by several effects, especially by the decreasing boiling point.

As can be seen by the boiler tray efficiencies in Table 3, there is no boiling in tray 18 for runs 4 and 6 and reduced boiling in tray 18 for run 7. This indicates that tray 18 was not needed to boil all the working fluid at those flows. In run 7, the size of tray 19 appears not to be large enough for the additional working fluid throughput. If both trays are considered together, the amount of heat which is transferred per hour in both of these trays increases with flow ratio (see Table 4), but the overall heat transfer coefficient decreases. This is understandable given the lower boiling point and larger pinch points causing the log mean temperature difference to increase. The overall heat transfer coefficient of the total tower preheating and boiling sections combined is not considered since it masks the effects of the pinch point.

The 60kW DCHX at Raft River compares favorably with several types of sieve plant tower heat exchangers. In Table 5, the 60kW has an overall heat transfer coefficient in the preheating section which is 1000 Btu/hr °F ft^3 greater than LBL's DCHX Spray Tower and is nearly 2000 Btu/hr °F ft^3 greater than Raft River's shell and tube heat exchangers (HX). The overall heat transfer coefficient for boiling in the sieve plant tower is five-times better than the other heat exchangers. The small pinch point, the well-derived heat transfer boiling region, and the large heat transfer area from bubbles and agitation attribute to this phenomenal number.

Conclusions

In conclusion, the thermal model provided a useful technique for analyzing the thermal hydraulic behavior of a sieve plate direct contact heat exchanger.

Preheater tray efficiencies increased with flow ratio indicating that jet formation of smaller droplets may be occurring, thus creating a greater heat transfer surface area per unit mass of working fluid. Observed tray efficiencies ranged from 50 to 70%.

The sieve plate direct contact heat exchanger performed well. Pinch points less than 0.1°F were obtained using 17 preheating trays; fewer trays would be required for an application in a power plant with this resource temperature.

Volumetric heat transfer coefficients were estimated to be approximately 20% higher for the preheating region of the sieve tray column than for a typical shell and tube heat exchanger or a spray tower, and about 500% higher than for spray columns or kettle boilers for the boiling region.

Footnotes

1. Based on 500 kW DCHX Pilot Plant Evaluation Testing, LBL-13339, Lawrence Berkeley Labs, October 1981.

Acknowledgement

The authors would like to acknowledge the greatly appreciated guidance of O. J. Demuth and J. F. Whitbeck.

TABLE 1. Experimental Conditions

Run #	Boiler Pressure, psia	Boiler Pressure, kPa	Boiler Temperature °F	Boiler Temperature °K	Working Fluid Flowrate lb/h	Working Fluid Flowrate kg/h	Geofluid Flowrate lb/h	Geofluid Flowrate kg/h
1	447	3,080	250	394	3,702	1,679	17,545	7,958
2	365	2,520	231	384	6,384	2,896	15,420	6,994
3	329	2,270	221	378	7,089	3,216	14,121	6,405
4	294	2,030	212	373	7,677	3,482	13,214	5,994
6	236	1,630	191	361	8,426	3,822	11,952	5,421
7	146	1,010	151	339	8,981	4,074	9,585	4,348

TABLE 2. Flow Ratios Which Best Fit the Experimental Temperatures

Run #	Experimental Flow Ratio working fluid out / geofluid out	Predicted Flow Ratio working fluid out / geofluid out	% Difference	Predicted Working Fluid Flow lb/h	Predicted Working Fluid Flow kg/h	Experimental Geofluid Flow lb/h	Experimental Geofluid Flow kg/h
1	.211	.230	∿ 9.0	4029	1828	17545	7958
2	.414	.433	∿ 5.0	6675	3028	15420	6994
3	.502	.524	∿ 4.0	7400	3357	14121	6405
4	.581	.583	∿ 0.2	7700	3493	13214	5994
6	.705	.744	∿ 5.0	8895	4035	11952	5421
7	.937	.985	∿ 5.0	9445	4284	9585	4348

TABLE 3. Tray Efficiencies Which Best Fit the Experimental Temperatures

Run #	Predicted Flow Ratio working fluid out / geofluid out	Distributor Tray Efficiency %	Preheater Tray Efficiency %	Predicted Pinch Point °F	Predicted Pinch Point °K	Boiler Tray Efficiency % Tray #18	Boiler Tray Efficiency % Tray #19
1	.230	61.5	50	.06	.03	97.6	92.5
2	.433	28.9	60	.09	.05	95.3	97.9
3	.524	38.1	65	.09	.05	99.3	97.3
4	.583	13.1	65	.13	.072	0.0	100.2
6	.744	15.0	70	.17	.094	0.0	99.5
7	.985	12.5	70	.36	.20	74.0	98.9

TABLE 4. The Amount of Heat Transferred and the Overall Heat Transfer Coefficients

Run #	Predicted Flow Ratio working fluid out / geofluid out	Distributor Tray Q_f*10^{-5} Btu/hr (watts)	Distributor Tray U_v Btu/hrft^3°F (watts/m^3°K)	Preheater Trays Q_f*10^{-5} Btu/hr (watts)	Preheater Trays U_v Btu/hrft^3°F (watts/m^3°K)	Boiler Trays Q_f*10^{-5} Btu/hr (watts)	Boiler Trays U_v Btu/hrft^3°F (watts/m^3°K)
1	.230	1.95	1045	2.84	3913	2.47	69,595
		(.571)	(19470)	(.832)	(72900)	(.724)	(1,296,600)
2	.433	.877	539	5.44	6348	5.38	69,115
		(.257)	(10000)	(1.59)	(118300)	(1.58)	(1,287,700)
3	.524	1.03	758	5.31	7340	6.43	65,965
		(.302)	(14100)	(1.56)	(136700)	(1.88)	(1,229,000)
4	.583	.305	227	5.87	7198	7.20	58,532
		(.0894)	(4230)	(1.72)	(134100)	(2.11)	(1,090,500)
6	.743	.252	282	5.19	8536	9.21	56,300
		(.0739)	(5250)	(1.52)	(159000)	(2.70)	(1,048,900)
7	.985	.085	212	3.13	8270	11.3	42,469
		(.0249)	(3950)	(.917)	(154100)	(3.31)	(791,200)

TABLE 5

U_v for RR 5MW Shell and Tube HX lb/hr °F ft^3 ($w/m^3 \cdot °K$)				U_v for LBL's 500 kW DCHX Spray Tower[1] lb/hr °F ft^3 ($w/m^3 \cdot °K$)		U_v for RR 60 kW DCHX Sieve Plate Tower lb/hr °F ft^3 ($w/m^3 \cdot °K$)	
Preheater		Boiler		Preheater	Boiler	Preheater	Boiler
L.P.	H.P.	L.P.	H.P.				
4529	4501	6897	7895	3500-7000	9375	4000-8500	40,000-70,000
(84,380)	(83,860)	(128,500)	(147,100)	(65,200-130,000)	(174,700)	(7,500-160,000)	(7,450,000-1,300,000)

DISCLAIMER